

Classification of Hyperspectral Images Compressed through 3D-JPEG2000

Ian Blanes¹, Alaitz Zabala², Gerard Moré³,
Xavier Pons^{2,3}, and Joan Serra-Sagristà¹

¹ Department of Information and Communications Engineering

² Department of Geography

³ Centre for Ecological Research and Forestry Applications (CREAF)

Universitat Autònoma de Barcelona

Cerdanyola del Vallès 08290, Spain

Ian.Blanes@uab.cat, Alaitz.Zabala@uab.cat, G.More@creaf.uab.cat,

Xavier.Pons@uab.cat, Joan.Serra@uab.cat

Abstract. Classification of hyperspectral images is paramount to an increasing number of user applications. With the advent of more powerful technology, sensed images demand for larger requirements in computational and memory capabilities, which has led to devise compression techniques to alleviate the transmission and storage necessities.

Classification of compressed images is addressed in this paper. Compression takes into account the spectral correlation of hyperspectral images together with more simple approaches. Experiments have been performed on a large hyperspectral CASI image with 72 bands. Both coding and classification results indicate that the performance of 3d-DWT is superior to the other two lossy coding approaches, providing consistent improvements of more than 10 dB for the coding process, and maintaining both the global accuracy and the percentage of classified area for the classification process.

Keywords: JPEG2000 standard, 3-dimensional coding, hyperspectral images, classification.

1 Introduction

With an ever increasing amount of data being gathered from the real world, the trend is that just a piece of them will only be used by the final application. This is the case in Remote Sensing, where it is a common practise to present data directly to a computer for it to perform an automatic process [1].

Still, since these data are valuable and expensive to produce, they need to be stored and distributed efficiently. To deal with the vast amounts of data gathered, compression is used. Lossy compression, *i.e.*, where compression performance is traded for quality, may be used if the decoder is still able to recover most of the relevant information. This relevant information is usually a small part of the whole image and can be coded efficiently. However, how much information loss can be allowed is application dependent.

In this paper we evaluate the influence of a lossy compression process on the computer-based classification of hyperspectral images. In the compression stage, basic JPEG2000 and 3-dimensional JPEG2000 [2] encodings have been considered.

This issue has been recently studied in the literature. In [3], the effects of the classic JPEG are examined on single component images. Later, effects of the new JPEG2000 on automated digital surface model extraction using aerial photographs are studied on [4]. And in [5], a JPEG and JPEG2000 comparison on single component is presented. In [6], classic JPEG, Vector Quantization, and a Wavelet-based compression technique are combined with a Karhunen-Loève Transform (KLT) to compare their effects on classification of 6-component imagery. In [7], the impact of using a Discrete Wavelet Transform (DWT) or a KLT with JPEG2000 is carefully examined, however they only present results for relatively small images.

Our work examines the performance penalty introduced due to the use of lossy compressed images (instead of the original images) on the classification process. Three distinct compression strategies are tested on a very large hyperspectral image obtained by a flight performed by the Cartographic Institute of Catalonia (ICC) using a Compact Airborne Spectrographic Imager (CASI) sensor. Due to the size of the data to compress, over 29 Gigabytes and 72 components, special care on constraining resources has had to be taken and some techniques could not be applied successfully (namely KLT). However, the three successfully tested techniques have been proved to be applicable in a production environment.

2 Material and Study Area

CASI and Laser Imaging Detection and Ranging (LIDAR) images over the Montseny area (a densely forested area on Catalonia) are used.

CASI is an optic sensor of hyperspectral scanning based on a small CCD bar that can be programmed to obtain a maximum of 288 bands among the 411 and 958 nm (red to near infrared). In this study a single image is used, recorded on 19-06-2007 (starting at 9.00 am) with 72 radiometric bands and an average bandwidth of 7.6 nm. The sensor flew on the airplane Cessna-Citation I from the ICC. The original image (without geometric correction) has 512 columns and 21133 rows. Lines captured by the sensor are affected by the movement of the airplane; therefore, it is necessary to geometrically correct the image line by line using a Global Positioning System (GPS) receiver and an Inertial Navigation System (INS). This geometric correction was made using the SISA system (developed by the ICC) [8]. Flight orientation is SW-NE, so the geometrically corrected image is very large (18366 columns and 11918 rows) and has a great proportion of NODATA pixels (only 3.98% of the image contains data pixels, see Fig. 1). Radiometric resolution of CASI images is unsigned 16 bits/pixel.

The airborne LIDAR is a sensor that consists of a laser and a mirror that diverts a beam in various directions perpendicularly to the trajectory of the airplane. These lateral displacements combined with the trajectory of the airplane

allow carrying out a ground sweeping. The system measures the distance from the sensor to the ground based on the time that the ray of light takes to reflect on the ground and reach back to the sensor. The result of a LIDAR flight is a collection of points with known coordinates. For every emitted pulse it can detect up to two echoes and for each of them register the reflected intensity. Over forested areas it is possible to obtain a Digital Terrain Model (DTM) and a Digital Vegetation Height Model (DVHM, *i.e.*, elevation of the vegetation covering the study area, obtained from the Digital Surface Model and the DTM). A Digital Slope Model (DSM) can be derived from the DTM. The original spatial resolution of the LIDAR images was 2 m, so they were resampled to 3 m to match the CASI resolution. The DTM had a range of 400-1500 m, the DVHM a range of 0-50 m while the DSM had a range of 0-100%. LIDAR-derived images were rescaled to a range similar to that of the CASI images in order to avoid under-representation during the unsupervised stage of classification.

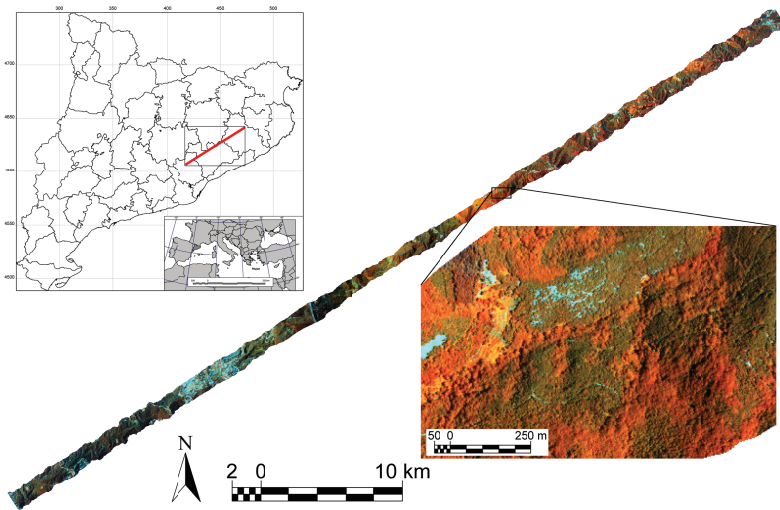


Fig. 1. RGB composition of bands 40 (707.3 nm), 66 (908.2 nm) and 12 (495.8 nm) of CASI image over Montseny (19-06-2007), area located in the western Mediterranean

3 Hyperspectral Coding

Among the many compression techniques now available to perform hyperspectral image compression [9,10,11], JPEG2000 is the most prominent one. JPEG2000 is the latest ISO image compression standard, that achieves very good compression results and provides a lot of other useful features, such as embeddedness and selective decoding. In addition, JPEG2000 has been devised to work in memory constrained environments.

Various techniques exist that perform a hyperspectral-aware compression, all generating a JPEG2000-compliant file. The following three have been tested in our experiments:

Band-Independent Fixed-Rate (BIFR)

In this method each hyperspectral band is independently compressed (in the sense that no inter-band redundancy is removed) and the bit-rate is equally split among all the hyperspectral bands. This approach reduces the encoder complexity and is suitable for memory constrained environments.

Volumetric Post-Compression Rate-Distortion (VolPCRD)

This technique may be thought of as the natural evolutionary step after BIFR. As in BIFR, bands still preserve inter-band redundancy, because no decorrelation transform has been applied. In this case though, rate is not equally shared, but “invested” where it helps to reduce further the distortion.

3 Dimensional Discrete Wavelet Transform (3d-DWT)

The DWT can be used as an inter-band decorrelation technique, allowing the removal of duplicate information across multiple bands (the 3rd dimension). This transform is applied on the input image, leading to an spectrally decorrelated image, and then a typical JPEG2000 compression follows in each band. Due to the nature of this method, an equally allocated rate must not be used, so the rate in the 3d-DWT must also be optimized.

All the presented techniques have in common that they allow selected zones of the images to be decompressed almost independently. This independence on the decoder is a very desirable characteristic, as a full decoding is a very memory and time consuming task. This allows human inspection of particular zones for human validation and improves the perceived decompression time.

Another well known technique exists, the KLT, where the optimal decorrelating linear transform is found for a Gaussian source. This search is extremely computationally expensive and not easily applicable on large images.

4 Classification

The classification is carried out with 72 bands of the CASI and with the DTM, the DVHM and the DSM obtained from the LIDAR data. Classification is performed on the CASI and the LIDAR images of forest land covers in order to obtain a land cover map with a six-category legend: *Fagus sylvatica*, *Castanea sativa*, *Quercus suber*, *Quercus ilex*, *Pinus halepensis*, and coniferous plantations. Combination between radiances (from CASI images) and topographic variables (from LIDAR images) improves the accuracy of the classification [12].

A mask obtained from the Land Cover Map of Catalonia (LCMC) was applied over the original and compressed images to only classify the forest areas. LCMC is a map obtained by means of photo-interpretation of 1:5000 color orthoimages captured in 2000, distinguishing up to 21 land covers.

A hybrid classification methodology is carried out using the MiraMon IsoMM and ClsMix modules [13]. The first part, IsoMM, is an IsoData implementation [14]. The second part of the hybrid classification is based on the ClsMix

MiraMon module. This module reclassifies each spectral class of an unsupervised classified image into thematic classes through spatial correspondence with training areas. The quality of this spectral to thematic class assignation is acquired with the use of two statistical thresholds called fidelity and representativeness. If the spatial correspondence between a spectral (obtained in the unsupervised stage) and a thematic (given by the supervised training areas) class does not fulfill both statistical thresholds, the spectral class will remain unclassified.

Training and test areas are obtained from field work (ground truth). From September to December 2007 the study area was visited several times and plots of forest inventory were generated (10 m radius parcels). This field work was complemented with digital photo-interpretation of 1:5000 color orthoimages of the ICC and ancillary data (Habitat Map of Catalonia, national forests inventories) to obtain areas of ground-truth. Thirty percent of those areas were reserved as independent test areas (to validate the final classification) and the remaining ones were used on the second part of the hybrid classification.

The obtained classification is validated using a confusion matrix between the classified image and the test areas reserved for this purpose.

5 Experimental Results and Discussion

5.1 Compression Results

The three reviewed coding approaches, BIFR, VolPCRD, and 3d-DWT, have been applied to encode the CASI image. Two distortion metrics have been computed, PSNR and SNR_Variance. Because of brevity, the coding performance is only reported for SNR_Variance, but PSNR results provide similar performance.

As expected, see Fig. 2a, 3d-DWT provides the best overall performance, followed by VolPCRD and then BIFR. When the distortion in individual bands is considered, see Fig. 2, all three approaches yield consistent results, improving the quality of the recovered image as the compression ratio (CR) increases (CR as compressed file size over uncompressed file size, NODATA pixels excluded in the uncompressed file size).

5.2 Classification Results

Global accuracy of the classification and percentage of classified area related to CR are shown in Fig. 3 and Table 1. As mentioned before, during the classification, the fidelity and representativeness parameters control the spectral to thematic class assignation. Spectral confusion can cause that some statistical classes remain unclassified, obtaining a classified area smaller than the total study area. Therefore, the classified area can be used as a quality index of the classification: the less the spectral confusion, the larger the classified area.

As could be expected, as CR decreases, the global accuracy also decreases. For high values of CR there are not important differences between compressed images and the images without compression. The decrease of global accuracy

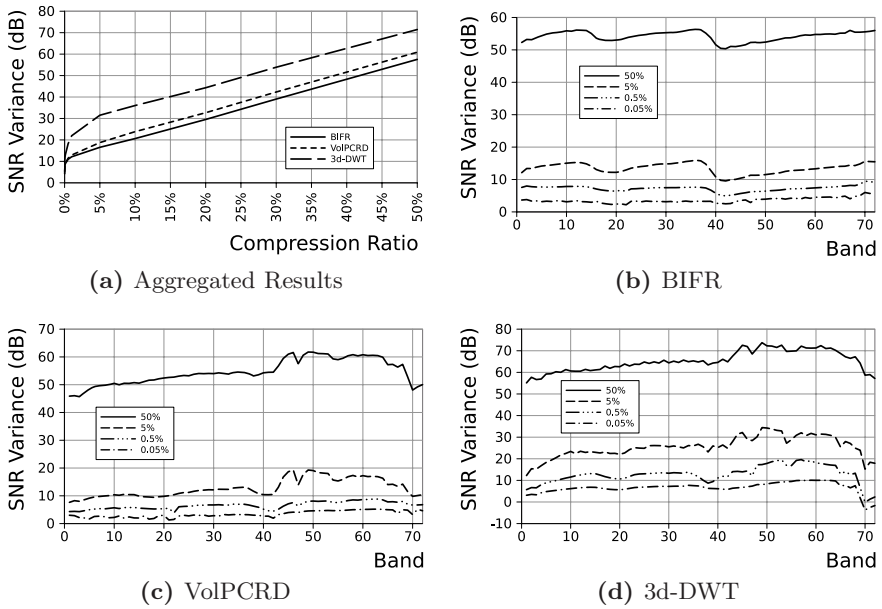


Fig. 2. Aggregated results of SNR_Variance over all components are shown in 2a. Per band results of the three studied methods are shown in 2b, 2c and 2d.

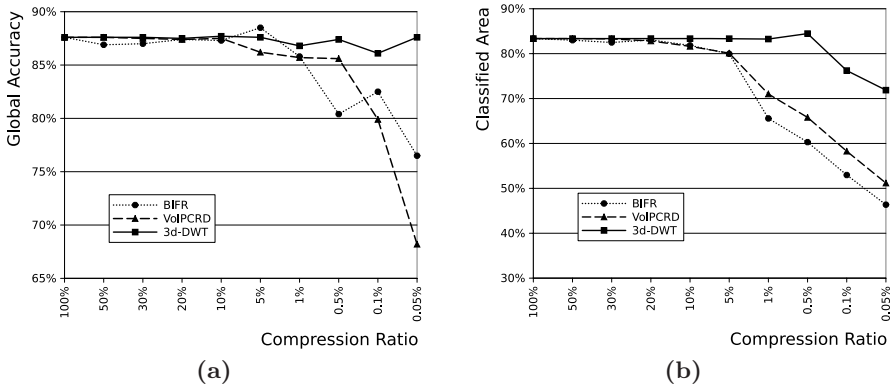


Fig. 3. Global accuracy (3a) and classified area (3b) of the obtained classifications using three compression techniques (BIFR, VolPCRD and 3d-DWT) related to CR

depends on the compression technique used. 3d-DWT brings the best results of global accuracy for the same CR values. According to classified area, the same tendencies are observed: there is no important influence when CR values are high, and 3d-DWT brings more classified area when CR values are low.

Table 1. Global accuracy of the obtained classifications and percentage of classified area using three compression techniques (BIFR, VolPCRD and 3d-DWT) related to CR

CR (%)	Global accuracy (%)			Classified area (%)		
	BIFR	VolPCRD	3d-DWT	BIFR	VolPCRD	3d-DWT
100.00	87.60	87.60	87.60	83.36	83.36	83.36
50.00	86.90	87.60	87.60	82.99	83.36	83.36
30.00	87.00	87.50	87.60	82.49	83.28	83.36
20.00	87.40	87.40	87.50	83.06	82.82	83.36
10.00	87.30	87.50	87.70	81.84	81.63	83.34
5.00	88.50	86.20	87.60	79.96	80.11	83.34
1.00	85.80	85.70	86.80	65.57	71.01	83.25
0.50	80.40	85.60	87.40	60.30	65.80	84.46
0.10	82.50	79.90	86.10	52.97	58.27	76.23
0.05	76.50	68.20	87.60	46.36	51.17	71.87

6 Conclusions

Modern sensors generate hyperspectral data at an unprecedented increasing pace. Coding techniques have to be devised to help disseminating and storing the sensed images; in order to improve the CR, lossy coding techniques are preferred over the lossless techniques. This approach poses the problem of assessing the influence of the compression process on an *a posteriori* classification process.

In this paper we investigate three JPEG2000-based lossy coding approaches: BIFR, VolPCRD, and 3d-DWT. 3d-DWT performs a DWT decorrelation in the spectral direction, and then a 2d-DWT in the spatial domain. After compression, a hybrid classification of the recovered images is performed. The hybrid classification combines an unsupervised module (IsoData), and a supervised module (ClsMix) that takes into account the spatial relationship among the thematic and spectral classes.

Experiments have been performed on a large hyperspectral CASI image with 72 bands. Both coding and classification results indicate that the performance of 3d-DWT is superior to the other two lossy coding approaches, providing consistent improvements of more than 10 dB for the coding process, and maintaining both the global accuracy and the classified area for the classification process.

Acknowledgments. This work was supported in part by the Ministry of Education and Science and the FEDER funds through the research projects Wavelet image compression for Remote Sensing and GIS applications (TIC2003-08604-C04) and Interactive coding and transmission of high-resolution images: applications in Remote Sensing, Geographic Information Systems and Telemedicine (TSI2006-14005-C02-01, TSI2006-14005-C02-02), and by the Catalan Government, under Grants 2008FI 473 and SGR2005-00319.

We would like to express our gratitude to the ICC for the availability of Remote Sensing data.

References

1. Jensen, J.: *Introductory Digital Image Processing. A Remote Sensing Perspective*. Pearson Prentice Hall, London (2005)
2. Taubman, D.S., Marcellin, M.W.: *JPEG 2000: Image Compression Fundamentals, Standards, and Practice*. Kluwer Academic Publishers, Dordrecht (2002)
3. Li, Z., Yuan, X., Lam, K.W.: Effects of JPEG compression on the accuracy of photogrammetric point determination. *Photogrammetric Engineering and Remote Sensing* 68(8), 847–853 (2002)
4. Shih, T.Y., Liu, J.K.: Effects of JPEG 2000 compression on automated dsm extraction: evidence from aerial photographs. *The Photogrammetric Record* 20, 351–365 (2005)
5. Zabala, A., Pons, X., Diaz-Delgado, R., Garcia, F., Auli-Llinas, F., Serra-Sagrasta, J.: Effects of JPEG and JPEG2000 lossy compression on remote sensing image classification for mapping crops and forest areas. In: *IGARSS 2006*, pp. 790–793. IEEE, Los Alamitos (2006)
6. Tintrup, F., De Natale, F., Giusto, D.: Automatic land classification vs. data compression: a comparative evaluation. In: *Proceedings of IGARSS 1998*, vol. 4, pp. 1751–1753. IEEE, Los Alamitos (1998)
7. Penna, B., Tillo, T., Magli, E., Olmo, G.: Transform coding techniques for lossy hyperspectral data compression. *IEEE Trans. Geoscience Remote Sensing* 45(5), 1408–1421 (2007)
8. Palà, V., Alamús, R., Pérez, F., Arbiol, R., Talaya, J.: El sistema CASI-ICC: un sensor multiespectral aerotransportado con capacidades cartográficas. In: *Revista de Teledetección, Asociación Española de Teledetección*, vol. 12, pp. 89–92 (1999)
9. Tang, X., Pearlman, W.A.: Three-Dimensional Wavelet-Based Compression of hyperspectral Images. In: *Hyperspectral Data Compression*, pp. 273–308. Springer, USA (2006)
10. Yeh, P.S., Armbruster, P., Kiely, A., Masschelein, B., Moury, G., Schaefer, C., Thiebaut, C.: The New CCSDS Image Compression Recommendation. In: *Aerospace Conference*, vol. 5–12, pp. 4138–4145. IEEE, Los Alamitos (2005)
11. Ramakrishna, B., Plaza, A., Chang, C.I., Ren, H., Du, Q., Chang, C.C.: Spectral/Spatial Hyperspectral Image Compression. In: *Hyperspectral Data Compression*, pp. 309–346. Springer, Heidelberg (2006)
12. Serra, P., Pons, X., Saurí, D.: Post-classification change detection with data from different sensors. Some accuracy considerations. *International Journal of Remote Sensing* 24(16), 3311–3340 (2003)
13. Pons, X., Moré, G., Serra, P.: Improvements on Classification by Tolerating No-Data Values. Application to a Hybrid Classifier to Discriminate Mediterranean Vegetation with a Detailed Legend Using Multitemporal Series of Images. In: *IEEE IGARSS and 27th CSRS, Denver*, pp. 192–195 (2006)
14. Duda, R.D., Hart, P.E.: *Pattern Classification and Scene Analysis*. John Wiley & Sons, New York (1973)